ELSEVIER

Biochimica et Biophysica Acta 1571 (2002) 225–238

BIOCHIMICA ET BIOPHYSICA ACTA
BBA

www.bba-direct.com

Evidence for binding of the ectodomain of amyloid precursor protein 695 and activated high molecular weight kininogen

Arpita Das [a,*], Neil R. Smalheiser [b], Adam Markaryan [a,1], Arnold Kaplan [a]

[a] *Department of Biological Sciences, University of Illinois at Chicago, Chicago, IL 60607, USA*
[b] *Department of Psychiatry, University of Illinois at Chicago, Chicago, IL 60607, USA*

Received 6 February 2002; received in revised form 2 May 2002; accepted 2 May 2002

Abstract

To identify ligands that bind to the N-terminal portion of human amyloid precursor protein (APP), we sought binding partners for a fragment of the ectodomain of human APP695 ($sAPP_{695}T$). The probe bound to fragments of high molecular weight kininogen (HK) in rat cortical membrane preparations in vitro. Laser confocal microscopy indicated that APP and HK colocalize near cerebral blood vessels, in the neuropil, and in many neurons of rat brain. $sAPP_{695}T$ bound to human activated kininogen (HKa) ($K_d = 0.3 \pm 0.1$ nM), but not to inactivated or low molecular weight kininogen. Binding was specific for the light chain sequence of HKa. Biotinylated human HKa also bound to $sAPP_{695}$ ($K_d = 0.3 \pm 0.5$ nM). $sAPP_{695}$ and HKa form tight complexes in solution that can be coimmunoprecipitated. These results support the hypothesis that forms of APP and kininogen can interact in brain tissue. Considering the implications of APP in neurite outgrowth, the APP–HKa interaction could modulate neurogenesis. © 2002 Elsevier Science B.V. All rights reserved.

Keywords: Amyloid precursor protein; Activated high molecular weight kininogen; Light chain of high molecular weight kininogen; Neuron; Binding

1. Introduction

Interest in the amyloid precursor protein (APP) began when it was shown to be the progenitor of beta-amyloid (Aβ). This peptide is present in plaques in the brains of Alzheimer's patients. Proteolysis of APP yields potentially toxic peptides, including Aβ 1–40 and Aβ 1–42. It also yields the soluble neurotrophin, sAPP [1–4]. This secretory product is nearly identical to the ectodomain of APP. APP is found in the cerebellum (dentate nucleus), cerebral cortex (layers III and V), hippocampus (pyramidal cell layer), and corpus callosum [5]. It is expressed in many brain cells including endothelial and meningeal cells, glia, astrocytes and neurons [6–9] and other cells [2]. In addition, sAPP is found in serum, plasma, and cerebrospinal fluid [10–13].

APP is a monotopic multifunctional transmembrane glycoprotein [14]. Many studies have sought APP binding proteins because it is felt that if two proteins interact with one another, they are probably involved in related cellular functions [15]. The C-terminal cytoplasmic domain of APP interacts with G-proteins [16], suggesting that it is a plasma membrane receptor. This domain also binds to APP-binding protein 1 (APP-BP1) [17], a cytoplasmic protein that is needed to move cells through the S–M checkpoint of their growth cycle [18]. The cytoplasmic tail of APP has also been shown to interact with several neuronal proteins such as FE65 [19], X11α [20], mDAB1 [21] and PAT1 [22]. Functions for these interactions have been proposed but not proven [23].

The ectodomain of APP was shown to tightly bind to extracellular matrix components, including collagen [24],

Abbreviations: HK, high molecular weight kininogen; HKa, activated high molecular weight kininogen; LK, low molecular weight kininogen; APP, amyloid precursor protein; $APP_{695}T$, truncated amyloid precursor protein isoform 695; Aβ, amyloidogenic peptide; sAPP, soluble amyloid precursor protein; PVDF, polyvinylidene difluoride; PAGE, polyacrylamide gel electrophoresis; DTT, dithiothreitol; HRP, horseradish peroxidase; PBS, phosphate-buffered saline; ELISA, enzyme-linked immunosorbent assay; TBST, Tris-buffered saline containing 0.05% TWEEN; CAPS, (3-[cyclohexylamino]-1-propanesulfonic acid) buffer; BB, binding buffer; BBT, binding buffer containing 0.05% TWEEN

* Corresponding author. Pharmacia, 4901 Searle Parkway, Bldg. Q 3624, Skokie, IL 60077, USA. Tel.: +1-847-982-7906; fax: +1-847-982-4226.

E-mail address: arpita.m.das@pharmacia.com (A. Das).

[1] Current address: Department of Microbiology and Immunology, University of Illinois at Chicago, Chicago, IL 60607, USA.

0304-4165/02/$ - see front matter © 2002 Elsevier Science B.V. All rights reserved.
PII: S0304-4165(02)00256-8

heparin sulfate proteoglycans [25–27] and laminin [28,29]. This specific adherence may play a role in the establishment of neurites and [2,30] may help APP function as a regulator of neuronal-cell or cell-matrix interactions [31]. To detect other APP-binding proteins we used a portion of the ectodomain of APP_{695} as our probe.

sAPP has both neuronal and non-neuronal functions (for reviews see Refs. [1–4]). The neuronal functions of sAPP include promotion of synaptogenesis and neurite outgrowth, regulation of synaptic plasticity, long-term potentiation, and neuroprotective effects [2]. The mechanisms by which sAPP mediates these neuronal effects remain unclear. Work from Saitoh's group [32] showed that specific sequences in sAPP could stimulate neurite outgrowth in tissue culture and improve memory when injected into the brains of living rats. This suggests that sAPP binds to a receptor or other proteins to mediate these effects. However, none of these proteins have been identified.

Hence, we sought proteins from rat cortex membrane preparations that bind to a biotinylated ectodomain fragment of an isoform of sAPP, $sAPP_{695}$, predominantly found in neurons. We chose it because we wished to avoid re-detection of proteases involved in blood clotting. The interaction of soluble forms of APP_{751} and APP_{770} with proteases has been well studied [31]. APP_{695} lacks the Kunitz Protease Inhibitor Domain and should not bind or inhibit proteases. Our preliminary studies [33] indicated that $sAPP_{695}$ can bind to a form of kininogen (HK) from rat membrane preparation in vitro.

HK is a multifunctional glycoprotein that undergoes complex proteolytic processing to yield activated kininogen (HKa) and the vasoactive nonapeptide, bradykinin [34–37]. HK plays a role in blood coagulation and angiogenesis. It down-regulates endothelial cell proliferation and migration [36] and binds to negative surfaces in a Zn^{++}-dependent fashion [38]. It is present in the brain in endothelial cells, meningeal cells, glia, astrocytes and neurons [39–41]. Li et al. [39] stressed the point that its functions in the brain are unknown.

HKa binds to membrane surfaces and receptors. HKa contains a histidine-rich region (domain 5) that interacts with the urokinase receptor and prevents the receptor from binding to vitronectin [35]. Domain 5 is also responsible for the anti-adhesive action of HKa on neutrophils [42–44] and endothelial cells [38,45,46]. The precursor of HK, HKa, has been shown to bind to proteins such as ferritin [47], thrombospondin [48], gC1q receptor [49], and heparin [50,51]. The physiological functions of these interactions are uncertain. Aggregated Aβ has been reported to bind to HK and play a role in the conversion of HK to HKa [52], producing high levels of HKa in the cerebrospinal fluid of Alzheimer's patients [53].

Here we provide evidence that the ectodomain of human $sAPP_{695}$ binds to the light chain of human HKa in a direct and specific manner. The results also indicate that forms of APP and HK colocalize in rat brain.

2. Materials and methods

2.1. Materials

Human HKa was purchased from Sigma Chemical Co., St. Louis, MO, or from their suppliers, Enzyme Research Laboratories, South Bend, IN. HK was purchased either from Enzyme Research Laboratories, or from Athens Research and Technology, Athens, GA. LK was purchased exclusively from Athens Research and Technology. Mouse monoclonal antibodies to either the light (C11C1) or heavy chain of HK were obtained from QED Bioscience, San Diego, CA, or, BioDesign International, Saco, ME. Monoclonal anti-APP m22C11 and polyclonal antibodies to peptides 44–63 and 99–126 of human APP were obtained from Chemicon, Temecula, CA. A C-terminal rabbit anti-APP polyclonal antibody, R1736, was a gift from Dr. Dennis Selkoe at Brigham and Women's Hospital, Harvard Medical School. Monoclonal antibody to protein tyrosine kinase [p-Tyr (Py20)] was obtained from Santa Cruz Biotechnology Inc., Santa Cruz, CA. A preparation of $sAPP_{695}$ prepared in a different strain of *Pichia pastoris*, using a different signal sequence [54] was a gift from Dr. Ikuroh Ohsawa from Japan. APP_{695} cDNA was a gift from Dr. Dennis Selkoe.

2.2. Preparation of secreted human recombinant $sAPP_{695}$ in *P. pastoris*

2.2.1. DNA manipulation and expression

DNA manipulations were performed as described in Ref. [55]. APP cDNA comprising nucleotides −2 to 2358 in expression vector pORFex13 [56] was a gift from Dr. Dennis Selkoe. DNA encoding the sequence from leu^{18} to lys^{613} of human APP_{695} was amplified by PCR. The following primers were used: 5′-CTGGAGCTACCCACTGAT-3′ (sense) and 5′-CTTCAAGTAGTAGTTTTTACT-3′ (antisense). The DNA fragment was gel-purified using a GeneClean II (Bio 101) kit, then cloned into the *Pml 1* site of the pPICZαB expression vector (Invitrogen), downstream of the *P. pastoris* alcohol oxidase (AOX1) promoter. The DNA of the cloned vector was sequenced to confirm that the insert was in frame with the α-factor secretion signal and the C-terminal tag. To transform *P. pastoris*, 10 μg of DNA were linearized with *Pme I*, mixed with *P. pastoris* strain SMD1168 (Invitrogen), and electroporated. Expression was induced by exposure to methanol for 29 h as described in the Invitrogen instruction manual.

2.2.2. Purification and biotinylation

After induction, the culture supernatant (200 ml) was filtered to remove any residual particles, and then loaded on a 5 ml heparin-Sepharose column (Amersham Pharmacia Biotech). The column was washed with 0.01 M sodium phosphate buffer, pH 7 until no protein was detected in the outflow. Then a 100 ml, 0–2 M linear NaCl gradient in 0.01 M sodium phosphate pH 7 buffer was applied to the column. The $sAPP_{695}$ content of the fractions was monitored by

Western blot analysis using monoclonal anti-APP antibody m22C11 and polyclonal antibody R1736. Fractions containing either $sAPP_{695}$ or $sAPP_{695}T$ were pooled, lyophilized and re-analyzed by SDS-PAGE. The C-terminal sequence of $sAPP_{695}T$ was obtained using a Procise C sequencer at the Mayo Protein Core facility, Mayo Clinic, Rochester, MN. The sequence we obtained, DDVLANM, is identical to amino acids 498–505 of APP_{695}. The biological activity of $sAPP_{695}$ and $sAPP_{695}T$ was confirmed in neurite outgrowth assays [32,57,58]. Purified $sAPP_{695}T$ was biotinylated using the Calbiochem kit, following procedures stated in the manufacturer's instruction manual. Commercial human HKa was biotinylated in the same way.

2.3. Blotting procedures

For dot blot analyses, samples were diluted in 20 mM sodium phosphate, 0.15 M NaCl [binding buffer (BB)]. Five-microliter aliquots were spotted on nitrocellulose transfer membranes (NitroBind, MSI Micron Separations Inc.) and allowed to air-dry. Non-specific binding sites were blocked with SuperBlock™ Blocking Buffer in TBS (Pierce). Blots were washed three times with 20 mM Tris, 136 mM NaCl, and 0.1% Tween-20 (TBST) pH 7.6. The blots were then incubated with either biotinylated $sAPP_{695}T$ or biotinylated HKa for 2 h at room temperature in 3% nonfat dry milk solution. Then, the membrane was incubated with a 1:40,000 dilution of avidin-horseradish peroxidase (avidin-HRP) (Sigma) in 3% nonfat dry milk for 2 h at room temperature. The membrane was washed with TBST. Bound probe was detected with a chemiluminescent substrate (ECL, Amersham Pharmacia Biotech) by flourography using Fuji RX film.

For ligand blotting, proteins were subjected to 10% SDS-PAGE by the Laemmli method [59] or wherever indicated to "Blue Native" gel electrophoresis [60,61]. Following electrophoresis, the gels were blotted onto polyvinylidene difluoride (PVDF) membranes (Millipore) overnight at 4 °C in 10 mM CAPS buffer (3-[cyclohexylamino]-1-propanesulfonic acid), pH 11, 10% methanol. Subsequently, the membrane was blocked with 3% nonfat dry milk for 2 h at room temperature, washed three times with TBST and incubated with biotinylated probe in 3% nonfat dry milk for 2 h at room temperature. The membrane was washed three times in TBST and incubated with a 1:40,000 dilution of avidin-HRP (Sigma) for 2 h at room temperature. In some cases, blots were incubated with monoclonal antibodies to either APP (m22C11) or HK (heavy chain) followed by secondary HRP-conjugated anti-mouse antibody (Amersham Pharmacia Biotech). Bound probe was detected as described for dot blots.

2.4. Preparation of rat brain membrane fractions

Membrane fractions were prepared from rat brain cortex by the procedure of Cohen et al. [62]. All procedures were performed at 4 °C. Briefly, whole rat brain cortexes from female Wistar rats (150–200 g) were homogenized with 10 volumes/gram wet weight of tissue in isolation medium A (0.32 M sucrose, 0.001 M $MgCl_2$, 0.05 mM $CaCl_2$, 1 mM $NaHCO_3$) containing Complete™ (Boehringer Mannheim) protease inhibitor cocktail tablets. The homogenate was centrifuged for 10 min at $1475 \times g$. The pellet was resuspended in isolation medium A and centrifuged again for 10 min at $755 \times g$. The combined supernatants were centrifuged for 10 min at $17{,}300 \times g$. The resulting "high-speed" supernatant was decanted and the pellet was resuspended in 3 ml/g of original tissue weight in isolation medium B (0.32 M sucrose, 1 mM $NaHCO_3$). This pellet was homogenized and layered on top of a step gradient composed of 6 ml each of 1.2, 1.0 and 0.85 M sucrose. The gradient was centrifuged for 120 min at $100{,}000 \times g$. Fraction 1 formed a band at the interface of the 1.0 and 1.2 M sucrose layers, fraction 2 between 0.85 and 1.0 M, and fraction 3 pelleted below the 1.2 M cushion. These fractions were separated and stored at −80 °C.

2.5. Protein purification and N-terminal sequencing

The fractions were treated with Triton-X-100 (0.005%) and subjected to 4–8% gradient "Blue Native" gel electrophoresis [60,61]. A ligand blot was performed and the $sAPP_{695}T$-binding bands were excised from the gel and eluted in 25 mM Tris–HCl, 192 mM glycine, 0.1% SDS buffer. The eluted proteins were dialyzed against water at 4 °C, lyophilized and dissolved in water. To determine the N-terminal sequence, the eluted proteins were subjected to SDS-PAGE (NOVEX), then blotted on to PVDF membranes using a CAPS buffer at pH 11. The protein bands of interest were excised and loaded on an Applied Biosystems (Foster City, CA) ABI-477A sequencer. Sequencing analysis was performed as recommended by Applied Biosystems.

2.6. ELISAs

To quantitate binding, wells of microtiter plates (MaxiSorb, Nunc) were incubated with $sAPP_{695}$, HKa, or HK in BB overnight at 4 °C. Wells were washed using a standard procedure, (three times with BB containing 0.05% Tween-20 (BBT) and three times with water). Subsequently, the wells were blocked with 3% milk solution for 1 h at 37 °C, and washed again. Biotinylated probe diluted in BB was added to each well for 2 h at room temperature. The solution was removed and washed by the standard procedure. Avidin-HRP (Sigma) at a 1:100,000 dilution was added to each well. After 2 h at room temperature, the solution was removed and the wells were washed again as described. Binding was detected with 0.2 ml per well of peroxidase substrate solution (5 mM Tris, 0.1 mM $CaCl_2$, pH 7.5, 0.01% H_2O_2, and 0.5 mg of *O*-phenylenediamine). The reaction was stopped by the addition of 25 μl of 3 M sulfuric acid and optical density

readings at 492 nm were recorded using an ELISA reader from Bio-Tech Instruments, Winooski, VT.

All ELISAs were optimized to minimize the variance and maximize the signal to background ratio. The average error of the mean was ± 7%. The extent of binding to wells coated with HKa or $sAPP_{695}$ forms was at least eight times the binding to wells containing no protein other than casein. In the absence of probe, binding was negligible either in the presence or absence of HK, HKa or $sAPP_{695}$.

2.7. Proteolytic processing of HK

HK (1.5 mg/ml) was incubated with plasma kallikrein (1 μg/mg of HK) in 0.1 M Tris–HCl, 0.15 M NaCl, pH 8.1, for 0–120 min at room temperature. At the indicated times, aliquots containing 2 μg of HK cleavage products were immediately treated with 2 × SDS–Laemmli buffer [59] containing 0.2 M DTT, boiled to inactivate kallikrein and analyzed by 10% SDS-PAGE and ligand blotting. For the dot blot analysis, aliquots containing 0.6 μg of reaction products were removed and the reaction was stopped with 10 mM benzamidine, 1 mM EDTA and 0.2 M DTT. The data was analyzed using the image analysis software SigmaScan Pro.

2.8. Coimmunoprecipitations

Reaction mixtures (0.5 ml) contained 0.5 μg of $sAPP_{695}$, 0.5 μg of $sAPP_{695}T$ and 1 μg of HKa, in classical phosphate-buffered saline (PBS) (137 mM NaCl, 2.7 mM KCl, 4.3 mM $Na_2HPO_4{\cdot}7H_20$, 1.4 mM KH_2PO_4, pH 7) with Complete™ (Boehringer Mannheim) protease inhibitor cocktail. Samples were cleared for 2 h with 20 μl of Protein G PLUS-agarose (Santa Cruz Biotechnology). Indicated antibodies were added, and the reaction mixtures were rocked at 4 °C for 2 h. Aliquots (20 μl) of Protein G PLUS-Agarose were added and the immunocomplexes were adsorbed by rocking the mixture at 4 °C for 2 h. The beads were collected by centrifugation for 10 s in the microcentrifuge and the supernatants were aspirated. The beads were washed two times with RIPA buffer (150 mM NaCl, 1.0% NP-40, 0.5% sodium deoxycholate, 0.1% SDS, 50 mM Tris, pH 8.0) and three times with PBS. The immunoprecipitates were solubilized in 30 μl aliquots of 2 × Laemmli sample buffer [59] containing 8% SDS. Aliquots (5 μl) of the supernatants were subjected to 10% SDS-PAGE and immunoblot analyses.

2.9. Colocalization

Adult rat brain was perfused with saline, fixed with 4% paraformaldehyde, post-fixed overnight, sectioned at 40 μ on a vibratome and microwaved for antigen recapture. Sections were blocked in 3% sheep serum/0.1% Triton X-100 in PBS for 1 h. Blocked sections were incubated at 4 °C overnight with primary antibodies (polyclonal anti-APP 1:1000, monoclonal anti-kininogen light chain 1:200, or both). After rinsing, secondary antibody (either anti-mouse FITC 1:200 and/or anti-goat—Alexa 546 1:500) were added for 2 h at room temperature and rinsed. As negative controls, some sections lacked primary antibody, or lacked antigen recapture, or were stained with a 1:300 dilution of monoclonal antibody against alpha-dystroglycan (Upstate Biotechnology, Inc.). Sections were covered with Fluoromount G (Southern Biotechnology Assoc.) and viewed at 630 × on a Leica laser scanning confocal microscope. To avoid bleed-through from one channel to the other, each channel was scanned separately. Each photo shown represents the average of eight sequential scans.

3. Results

3.1. $sAPP_{695}T$ binds to fragments of HK in rat brain membranes in vitro

Recombinant forms of human APP_{695} were purified from a protease deficient strain of *P. pastoris* as described in Materials and methods and by the following groups: in Refs. [54,63,64]. The yeast secreted a full-length 95 kDa ($sAPP_{695}$) and a truncated 68 kDa form ($sAPP_{695}T$). C-terminal analysis revealed it to be truncated at amino acid 505 (see Materials and methods). Both forms stimulated neurite outgrowth from rat neuronal B103 cells [32,57,58]. A preparation of highly purified $sAPP_{695}T$ was biotinylated for use as the probe in binding studies.

This probe bound tightly to proteins from subfractions of rat brain membranes. The binding proteins were partially purified from the subfractions by "Blue Native" gel electrophoresis. Two clusters of binding proteins ("I" and "II") were detected (Fig. 1A). Each cluster was eluted. Each retained its ability to bind to $sAPP_{695}T$. No sequences were obtained from cluster "I". Therefore, only $sAPP_{695}T$ binding to eluted cluster "II" is shown in Fig. 1B Cluster "II" was subjected to SDS-PAGE. Its two main components (α and β) have apparent molecular weights of 73 and 44 kDa as shown in Fig. 1C. Their N-terminal peptide sequence was obtained. In both cases, the sequence was "NNATFYFKID." A nearly identical sequence, "NNHTFYFKID," is present at amino acid 293–302 of rat HK (Medline accession number 87137465). A cartoon of the likely structure of the HK fragments is shown in Fig. 1D. The cartoon is based on their molecular weights as estimated from their mobility, and the location of the sequence determined above. These inferred structures are predominantly composed of HK light chain sequence. The results suggested that APP or sAPP might bind to HK or HKa in rat brain. This is why we wished to determine if the two proteins colocalize in the brain.

3.2. APP and HK colocalize in rat brain

Rat frontal cortex and hippocampus were double-labeled with a monoclonal anti-HK (light chain) antibody that recognizes both HK and HKa, and an N-terminal polyclonal

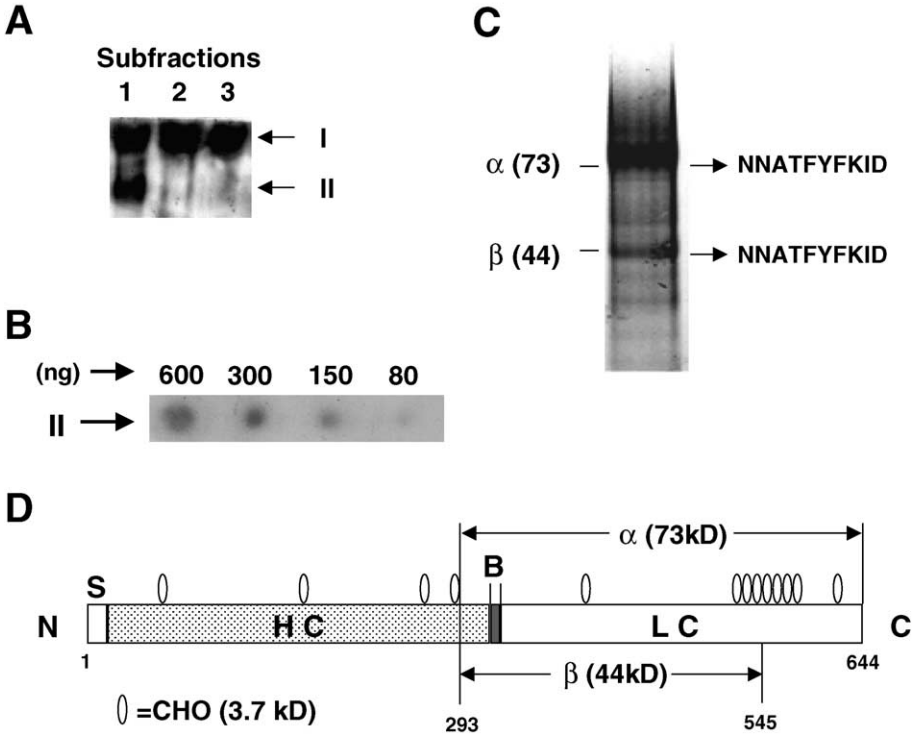

Fig. 1. $sAPP_{695}T$ binds to fragments of HK in rat brain membrane subfractions in vitro. (A) Proteins from rat brain subfractions that binds $sAPP_{695}T$. Rat brain was homogenized and subjected to sucrose gradient centrifugation as described in Materials and methods. Subfraction 1 banded at the interface between 1.0 and 1.2 M sucrose; subfraction 2 between 0.85 and 1.0 M. Subfraction 3 pelleted below the 1.2 M cushion. Five micrograms of each were subjected to "Blue Native" gel electrophoresis [60,61]. The proteins were transferred to a PVDF membrane and a ligand blot was performed using 10^{-8} M biotinylated $sAPP_{695}T$. Protein bands "I" and "II" of subfraction 1 were excised, eluted and further analyzed for $sAPP_{695}T$ binding activity. (B) Binding of $sAPP_{695}T$ to eluted cluster "II". Protein from eluted cluster "II" was spotted on a nitrocellulose membrane at the indicated concentrations and probed for binding to 10^{-8} M biotinylated $sAPP_{695}T$. (C) Components of mixture "II" contain kininogen fragments. Eluted proteins from mixture "II" were subjected to 4–12% gradient gel electrophoresis (NuPAGE Bis–Tris). The bands indicated as "α" and "β" were excised and subjected to N-terminal sequencing as described in Materials and methods. (D) Model of kininogen fragmentation. "N" is amino-terminus, "S" is signal sequence, "B" is bradykinin sequence, "HC" is heavy chain, "LC" is light chain and "C" is carboxy-terminus. The "CHO" represents potential N- or O-linked glycosylation sites. The total apparent mass of oligosaccharide residues was estimated by subtraction of the inferred mass of the protein sequence (73 kDa) from the apparent mass of the glycosylated protein (120 kDa) on the gel. The average mass per oligosaccharide (3.7 kDa) was estimated by dividing the inferred oligosaccharide mass (48 kDa) by the number of potential glycosylation sites, 13.

anti-APP antibody that recognizes all isoforms of APP and sAPP. These were viewed by laser scanning confocal microscopy.

After antigen recapture, anti-HK (light chain) antibody heavily decorated the basal laminae surrounding some of the larger blood vessels (Fig. 2A, left). To mark basal laminae, an antibody against alpha-dystroglycan was employed. It reliably decorated all basal laminae within these brain sections, both with and without antigen recapture (data not shown). Because antigen recapture was necessary to expose the kininogen epitope, some of the kininogen signal may have gone undetected. The antibody also labeled the pial surface of the brain (not shown). Anti-APP labeled many of the same sites (Fig. 2A and B, middle).

A set of neuronal cell bodies was labeled with anti-HK (light chain) (Fig. 2C, left). These were predominantly larger cells that appeared to be pyramidal neurons. There was occasional staining of the neurites of these cells. Lighter diffuse labeling of neuropil was also detected. Anti-APP intensely labeled the cell bodies and proximal dendrites of larger neurons (Fig. 2C, middle). The cells with large nuclei (probably glia) are also labeled with both anti-APP and anti-HK. These findings are in consonance with reports that kininogen [39,40] and APP [6–9,65] are expressed in large neurons and glia.

When the left and middle panels in Fig. 2 were overlaid, striking colocalization of the two antibodies was observed around blood vessels, in neuronal and glial cell bodies and in small punctate spots within the neuropil (Fig. 2A, B and C, right). However, anti-APP did not always colocalize with anti-HK. Colocalization was observed only on discrete portions of basal laminae and perivascular regions (Fig. 2A and B, right). Neurons were found which were positive only for anti-HK (light chain) staining. Others were positive only for anti-APP staining (data not shown). These results suggest that some, but not all, of the tissue pools of HK and APP are colocalized within 1 μ of each other. However, colocalization studies cannot easily differentiate between proximity, presence in a multicomponent complex, and direct interaction.

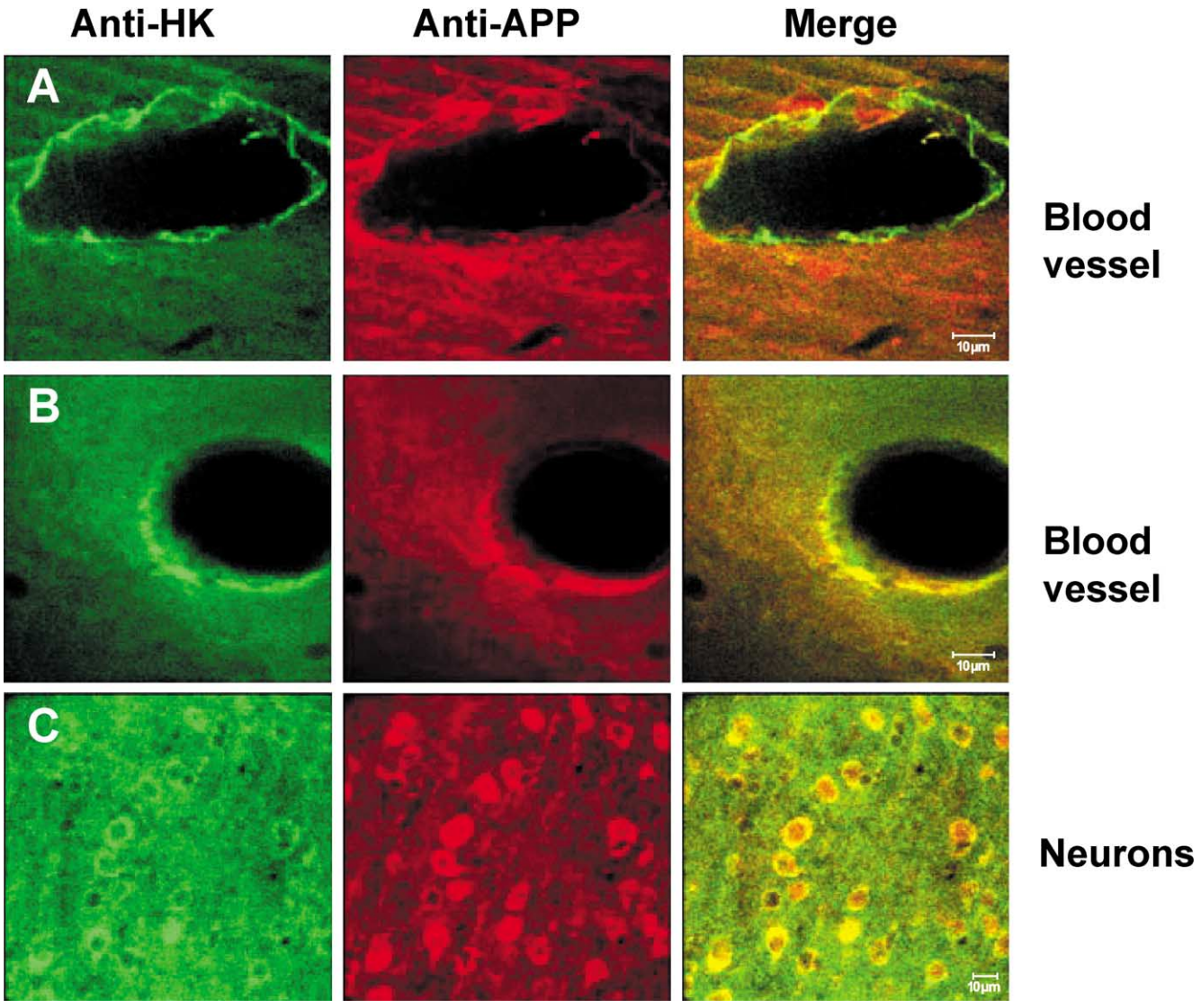

Fig. 2. Colocalization of APP and HK in adult rat frontal cortex using confocal microscopy. A and B are immunostained regions in the vicinity of blood vessels. C is an immunostained layer of frontal cortex, showing colocalization of staining in neuronal cell bodies and neuropil. The green images shown in the left panels are immunostained for kininogen, as described in Materials and methods. The red images shown in the middle panels are immunostained for APP. Those in the right panels represent overlays. Yellow color appears at sites of colocalization.

3.3. Interaction between human $sAPP_{695}$ and HKa is direct and specific in vitro

Evidence for direct binding can come from analysis of mixtures of pure proteins. To evaluate binding, we employed a variety of assays, including dot blot, ligand blot, and coimmunoprecipitation. As shown in Fig. 3A, $sAPP_{695}T$ exhibited an ability to bind native HKa in dot blots but much less ability to bind to native HK. Binding to LK could not be detected. The light chain amino acid sequence, 428–644, is present in HKa and HK, but absent in LK [66], suggesting that an HK light chain sequence is required for $sAPP_{695}T$ binding.

The observed difference in binding of $sAPP_{695}T$ to HK and HKa (Fig. 3A) might be caused by artifactual differences in their commercial preparations. To eliminate that possibility, we measured binding to the same HK preparation, before, during and after its conversion to HKa (Fig. 3B). The amount of $sAPP_{695}T$ binding was quantitated with the help of the accompanying standardization (Fig. 3C). A 5-fold increase in binding capacity was observed during the first 15 min of treatment with kallikrein. This confirms the idea that the difference between HK and HKa binding observed in Fig. 3A is due to their structure.

The analysis in Fig. 4 supplies further evidence for the role of light chain sequences as binding sites. HK was treated with plasma kallikrein under the same conditions as described in Fig. 3B, then subjected to SDS-PAGE and binding analysis. Coomassie staining (Fig. 4A) revealed that HK was converted to heavy chain, transient light chain intermediate and light chain. Tayeh et al. [67] reported

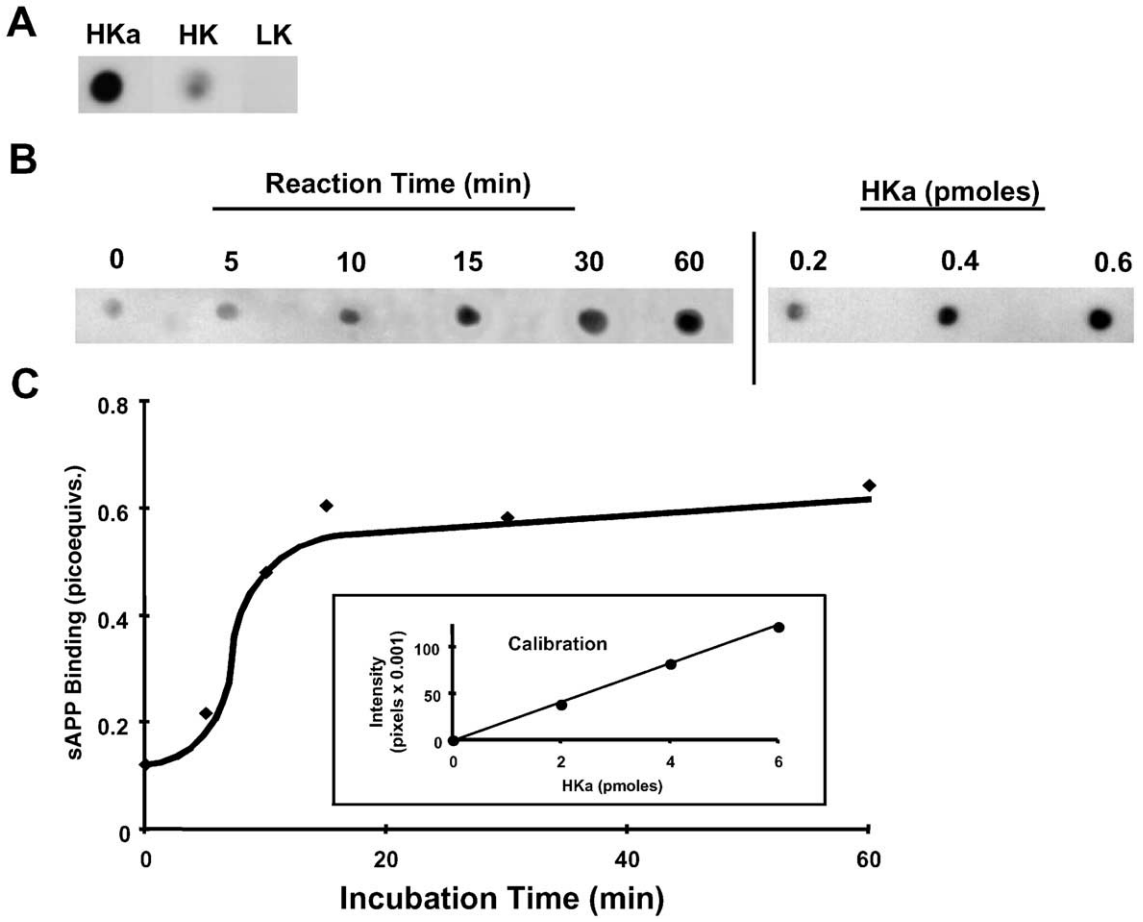

Fig. 3. Interaction of human HK forms with recombinant human $sAPP_{695}T$. (A) $sAPP_{695}T$ binds to HK forms. Samples containing 0.3 μg of human HKa, HK, or LK were spotted on a nitrocellulose membrane. Binding of 10^{-8} M biotinylated $sAPP_{695}T$ to the blots was detected as described in Materials and methods. (B) Effect of plasma kallikrein treatment on $sAPP_{695}T$ binding. Human HK (1.5 mg/ml) was incubated with kallikrein (1 μg/mg of HK) at pH 8.1 and room temperature. At times indicated, aliquots containing 0.6 μg of reaction products were stopped with 10 mM benzamadine, 1 mM EDTA and 0.2 M DTT. The samples were spotted on a nitrocellulose membrane and probed with 10^{-8} M biotinylated $sAPP_{695}T$. For the calibration curve samples containing the indicated concentrations of human HKa were spotted on a nitrocellulose membrane in the presence of 0.2 M DTT and probed with 10^{-8} M biotinylated $sAPP_{695}T$ as described in Materials and methods. (C) Effect of plasma kallikrein treatment on binding of $sAPP_{695}T$ to HK cleavage products. This was determined by densitometric analysis of dot blots in (B). Inset: calibration curve. Band intensities were expressed as picoequivalents of HKa. A picoequivalent is the amount of intensity obtained (as pixels) from binding of $sAPP_{695}T$ to 1 pmol of HKa under the described conditions. The experiment was repeated at least three times and representative results are shown.

similar results and identified the intermediate band as a mixture of two C-terminal fragments of HK.

A blot of an identical gel was probed for $sAPP_{695}T$ binding and the staining was calibrated with the accompanying standards (Fig. 4B). A quantitation of the results is presented in Fig. 4C. During the first 30 min, all binding to HK disappeared. This corresponded to the disappearance of HK itself (Fig. 4A). The heavy chain did not bind to $sAPP_{695}T$. By 30 min, essentially all the binding was produced by light chain intermediate and product. By 2 h, the bulk of binding could be attributed to the light chain. This was 3-fold greater than that of the original HK. During the period from 30 to 120 min, little effect was observed on total binding. This occurred in spite of the conversion of intermediate to end product, suggesting that the available light chains of intermediates and products bound to $sAPP_{695}T$ with roughly equal capacity. The binding of thrombospondin to HK forms during kallikrein treatment exhibited a similar specificity [48].

We next evaluated the possibility that HK binding was qualitatively different from HKa binding with ELISAs. As shown in Fig. 5, biotinylated $sAPP_{695}T$ bound to HKa in a saturable fashion at low concentrations. At higher concentrations, a further non-saturable element of the binding was evident (data not shown). On the other hand, binding to HK was a linear function of probe concentration at all concentrations tested. $sAPP_{695}T$ binding to HKa was 10-fold that of HK at 1 nM and 2.5-fold at 6 nM. These ratios are similar to those obtained from dot blot analyses (Fig. 3). We calculated an apparent K_d of 0.3 ± 0.1 nM by regression analysis. A similar apparent K_d of 0.3 ± 0.05 nM was obtained when the binding was done in reverse (biotinylated HKa to unlabeled $sAPP_{695}$) (data not shown).

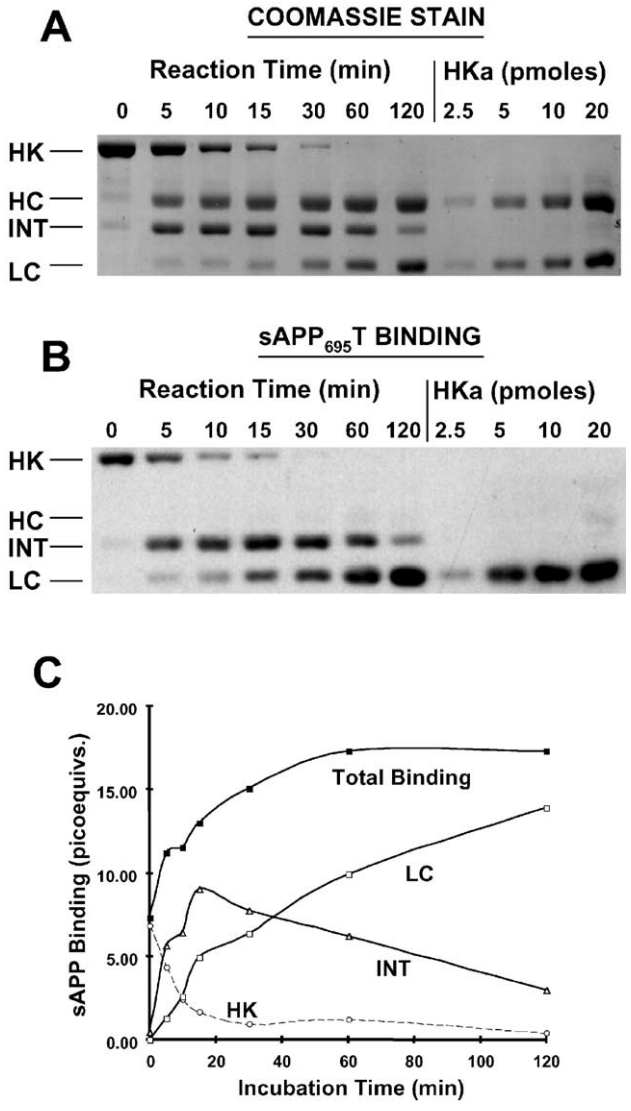

Fig. 4. SDS-PAGE analysis of human HK cleavage by plasma kallikrein. (A) Coomassie stain. Human HK (1.5 mg/ml) was incubated with kallikrein (1 μg/mg of HK) at pH 8.1 at room temperature. At times indicated, aliquots containing 2 μg of HK cleavage products were stopped, subjected to 10% SDS-PAGE and Coomassie stained to visualize bands. The positions of HK, heavy chain (HC), light chain containing intermediate (INT) and light chain product (LC) are indicated. The indicated amounts of human HKa standards were also subjected to SDS-PAGE. (B) $sAPP_{695}T$ binding to the HK cleavage products. A duplicate of the gel described in (A) was subjected to 10% SDS-PAGE. The gel was blotted on a PVDF membrane. A ligand blot was performed, using 10^{-8} M biotinylated $sAPP_{695}T$. Bound biotinylated $sAPP_{695}T$ was detected with avidin-HRP as described in Materials and methods. (C) Progress curves for the processing of HK. These were determined by densitometric analysis of the ligand blot shown in (B). Band intensities were expressed as picoequivalents of HKa. "Total Binding" is the sum of values for "HK", "INT" and "LC". The experiment was repeated at least three times and representative results are shown.

3.4. HKa binds equally well to $sAPP_{695}$, $sAPP_{695}T$ and biotinylated $sAPP_{695}T$

The observed binding of biotinylated $sAPP_{695}T$ to HKa could be the result of either the attached biotin group or an artifact caused by truncation of $sAPP_{695}$. A common way to eliminate these possibilities is to compare the potency of inhibition ($[I]_{50}$) by compounds to the K_d of the probe. Fig. 6 shows that the binding of biotinylated probe was inhibited by addition of unlabeled $sAPP_{695}T$ and by unlabeled $sAPP_{695}$ from two different sources. One of these is full-length $sAPP_{695}$ purified as described in Materials and methods. The other is from a different strain of *P. pastoris*, using a different promoter and purified in a different way [54]. The inhibition curves for the three unlabeled preparations overlapped. The $[I]_{50}$s for the three preparations (0.1–1 nM) were not significantly different from the apparent K_d of biotinylated $sAPP_{695}T$ or from each other. The purity of the $sAPP_{695}$ preparations (greater than 95% in each case) is shown in the inset to the figure. Labeled $sAPP_{695}T$ was slightly less mobile than its unlabeled form. Binding was also inhibited 50–70% by coating wells that contained HKa with unlabeled $sAPP_{695}T$ before initiating the binding reaction (data not shown).

3.5. HKa and $sAPP_{695}$ coimmunoprecipitate

In the assays described above, reactions were performed with one binding partner fixed on a substratum and the other biotinylated. In the experiment described in Fig. 7, $sAPP_{695}$, $sAPP_{695}T$ and HKa were in solution and were not labeled. Aliquots were immunoprecipitated with a monoclonal anti-APP (m22C11), anti-HKa (heavy chain) monoclonal anti-

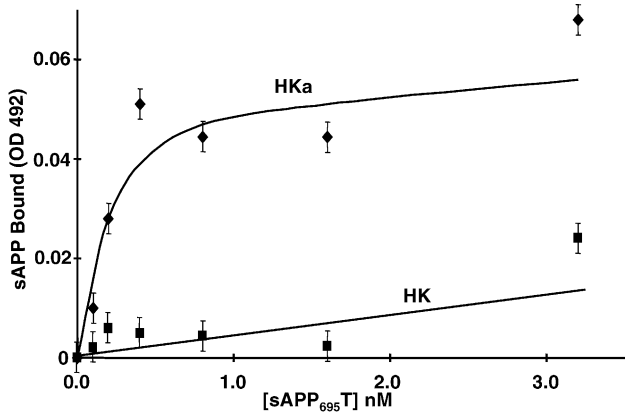

Fig. 5. Effect of human recombinant $sAPP_{695}T$ concentration on binding to human HKa and HK. The wells of microtiter plates were coated with 0.2 ml of either 20 μg/ml HKa or HK (see Materials and methods). The coated wells were incubated with the indicated concentrations of biotinylated $sAPP_{695}T$. Bound biotinylated $sAPP_{695}T$ was measured at OD 492 nm after wells were treated with avidin-HRP and HRP substrate solution. Background readings were obtained for the indicated biotinylated $sAPP_{695}T$ concentration in wells coated with no HK or HKa. These background values were subtracted from the total binding values obtained from wells coated with either HK or HKa to obtain net binding. Each value was obtained at least in duplicate, on six different occasions and representative results are shown. Error bars reflect mean standard deviations of $\pm$ 7%. A least squares fit of the data to a rectangular hyperbola was determined by regression analysis using Sigma Plot software. The apparent K_d for $sAPP_{695}T$ binding to HKa was determined to be 0.3 ± 0.1 nM ($R^2 = 0.90$).

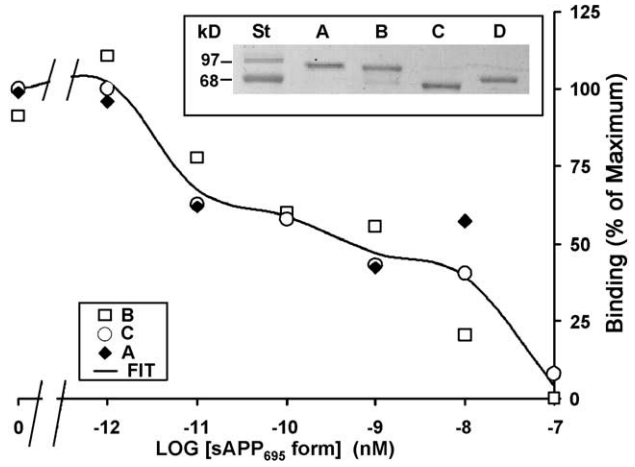

Fig. 6. Effect of unlabeled $sAPP_{695}$ forms on binding. Microtiter wells were coated with HKa (10 μg/ml), then incubated with biotinylated $sAPP_{695}T$ (10^{-8} M) in the presence of one of the following unlabeled proteins at the indicated concentrations (A) $sAPP_{695}$ (Ohsawa et al. in Ref. [54]), (B) $sAPP_{695}$, and (C) $sAPP_{695}T$. "Fit" represents the best-fit curve for all the data points. Binding values were obtained by correcting for background as described in Fig. 5. To obtain the percentage of maximal binding, the binding values were divided by the value at zero inhibitor added, then multiplied by 100. Each value was obtained at least in triplicate. Inset: SDS-PAGE of $sAPP_{695}T$ samples. One microgram each of (A) $sAPP_{695}$ (Ohsawa et al. in Ref. [54]), (B) $sAPP_{695}$, (C) $sAPP_{695}T$, and (D) biotinylated-$sAPP_{695}T$ were subjected to 10% SDS-PAGE and Coomassie stained to visualize bands.

body, no antibody, or irrelevant monoclonal antibody (anti-tyrosine kinase). Anti-HK (light chain) antibody was a poor immunoprecipitant and no results were obtained. As shown in Fig. 7A (lane 1) immunoprecipitates prepared using m22C11 contained the expected full-length (95 kDa) and truncated (68 kDa) $sAPP_{695}$. They were also present when immunoprecipitates were prepared with anti-HKa heavy chain (lane 2). They were barely detectable in control lanes (lanes 3–5). As shown in Fig. 7B, immunoprecipitates probed with anti-HKa (heavy chain) contained the expected 95 kDa two-chain form of HKa (lane 7). The 95 kDa form also immunoprecipitated when m22C11 (lane 6) was employed. It was not brought down by irrelevant antibody (lane 9) or other controls (lanes 8 and 10). When this band was subjected to SDS-PAGE under reducing conditions, its molecular weight shifted to 55 kDa (data not shown). This was expected since the 95 kDa HKa is converted to heavy (55 kDa) and light (43 kDa) chains upon reduction. Bands were also detected at 29 kDa. These are not shown because they also appeared when only secondary antibody was used. The results indicate that $sAPP_{695}$ and HKa form relatively tight complexes in solution.

3.6. Binding occurs at physiological pH and NaCl concentration

As shown in Fig. 8A, the observed pH profile (Fig. 8A, I) indicates an apparent pH optimum between 6 and 7 and a secondary peak at pH 5. However, the extent of HKa desorption from wells is directly dependent on the pH (Fig. 8A, II). After correction for this dependency (Fig. 8A, III) an optimum near pH 5 and a shoulder at pH 6 and 7 becomes apparent. This suggests the capability for binding at either extracellular or endosomal pH. As shown in Fig. 8B, binding to HKa was optimal at physiological ionic strengths, unaffected by hypertonic NaCl, but lessened at hypotonic NaCl. Binding was inhibited 70% in the presence of 0.2 M dithiothreitol (DTT), but unaffected by 5 and 10 μM EDTA, EGTA, Ca^{+}, Mg^{+}, or Mn^{+} (data not shown). Binding was also unaffected by 5 and 10 μM Zn^{+} (data not shown), indicating that binding of $sAPP_{695}T$ to HKa is not Zn^{+}-dependent. Not all proteins that bind to HK/HKa require the presence of Zn^{+}.

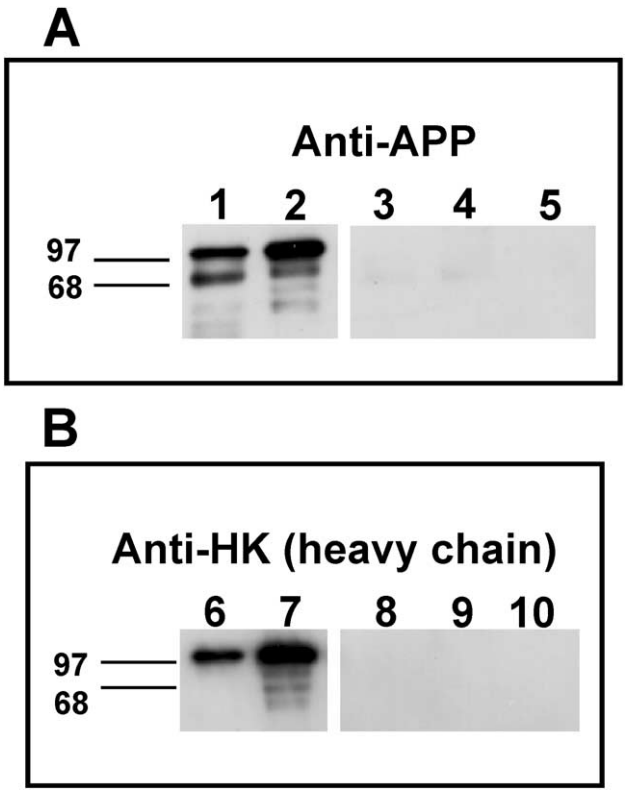

Fig. 7. Coimmunoprecipitation of a mixture of $sAPP_{695}$, $sAPP_{695}T$ and HKa. As described in Materials and methods, a mixture containing 0.5 μg $sAPP_{695}$, 0.5 μg $sAPP_{695}T$, and 1 μg of HKa were mixed and immunoprecipitated with antibodies and Protein G beads. The coated beads were washed, solubilized in SDS sample buffer and subjected to 10% SDS-PAGE. Lanes contained extracts derived from immunoprecipitates prepared with the following antibodies: lane 1, monoclonal anti-APP antibody (2.5 μg); lane 2, monoclonal anti-HK (heavy chain) antibody (5 μg); lane 3, no antibody; lane 4, monoclonal anti-p-Tyr antibody (1 μg). The sample in lane 5 contained PBS buffer, but no $sAPP_{695}$, $sAPP_{695}T$, HKa or antibody. It was treated with Protein G like the samples in lanes 1–4. Lanes 6–10 contained immunoprecipitates identical to those in lanes 1–5 that were loaded on a separate gel. The immunoprecipitated proteins were analyzed by Western blot using either monoclonal anti-APP (A) (lanes 1–5), or monoclonal anti-HK (heavy chain) antibody (B) (lanes 6–10). The experiment was repeated on three different occasions and representative gels are shown.

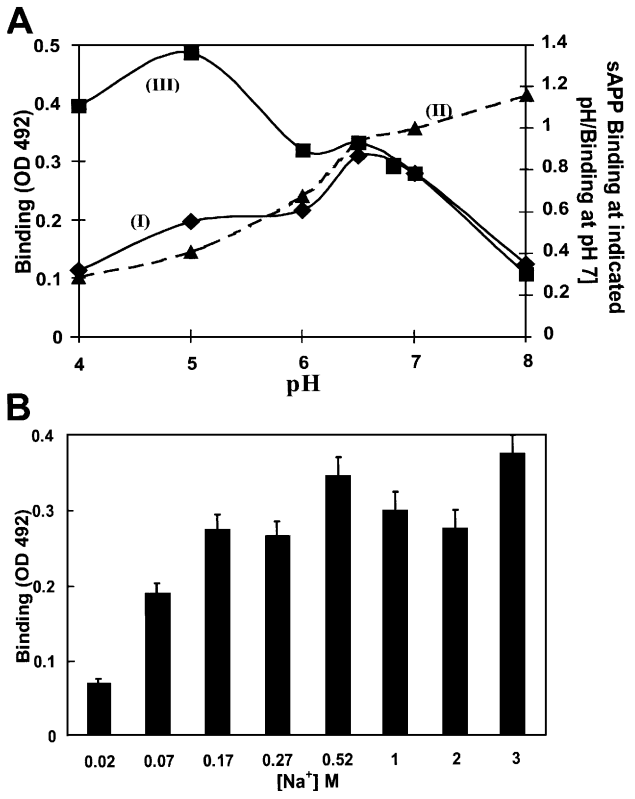

Fig. 8. Effect of pH and NaCl concentration on binding. In each case, the probe was 10^{-8} M biotinylated $sAPP_{695}T$ and the wells were coated with 10 μg/ml HKa as described in Materials and methods. The readings obtained in wells that were not coated with HKa were subtracted from the total. Each value was obtained at least in triplicate, on two different occasions and then averaged. Error bars reflect mean standard deviations of ± 7%. The bars were omitted from (Fig. 8A) to avoid figure clutter. (A) pH profile. Microtiter wells coated with HKa were incubated with biotinylated $sAPP_{695}T$. The probe was diluted in one of the following buffers: 20 mM sodium acetate buffer, 0.15 M NaCl pH 4, 5 or 6; or BB adjusted to either pH 6.5, 7 or 8. The results are shown in (I). To account for the effects of pH on HKa desorption, coated wells were first incubated at the indicated pH for 2 h at room temperature then washed and assayed for binding at pH 7. Values obtained at each pH treatment were divided by the value obtained at pH 7. The ratios are shown in (II). The calculated values shown in (III) were normalized for HKa binding to wells at pH 7 by dividing the observed values in (I) by the ratios in (II). (B) NaCl effects. To test the effects of NaCl concentration on binding of $sAPP_{695}T$ to HKa, wells coated with HKa were incubated with probe at the indicated NaCl concentrations. No effect of NaCl concentrations on HKa desorption was observed.

Binding of HK to ferritin [47] and HK to thrombospondin [48] have not been reported to be Zn^{+}-dependent

4. Discussion

Our results provide good evidence for the following conclusions: (a) forms of APP and HK colocalize in rat brain near large cerebral blood vessels and in a set of neurons. (b) $sAPP_{695}$ and HKa directly interact with each other in a specific and saturable manner in vitro.

Our search for $sAPP_{695}$ binding proteins in rat cortex membrane preparations led to the detection and isolation of putative kininogen fragments. Their identification was based, in part, on their N-terminal amino acid sequence. The same sequence was obtained from two fragments of cluster "II" (Fig. 1C). It was 90% identical to a 10-amino acid sequence present near the end of the heavy chain of rat HK (amino acid 293–302). We also inferred from this sequence and their estimated molecular weights that the fragments were predominantly comprised of HK light chain. Data from this in vitro binding experiment implied that APP could bind to HK in rat brain.

To gather more evidence for this idea, we performed colocalization studies in rat brain using confocal laser microscopy. The confocal microscopy studies in Fig. 2 indicate that antibody reactive forms of APP and HK are close to each other on specific cerebral extracellular matrices, in some neurons and near some large blood vessels. Colocalization studies in rat brain using transmission electron microscopy showed that in some neurons, HK and APP can be as close as 5 nm (data not shown). These colocalization studies support the idea of an interaction. However, with these techniques, it is very difficult to differentiate between mere proximity, presence in multiprotein complexes and direct binding.

We then performed direct binding studies in vitro. The tight binding of the $sAPP_{695}T$ probe to human HKa (Figs. 3–6) and of the HKa probe to $sAPP_{695}$ (data not shown) indicated that human $sAPP_{695}$ and HKa can form direct binding complexes. Since binding was shown on ELISA plates, dot blots, ligand blots and by coimmunoprecipitation from solution, the evidence for this seems robust. Coimmunoprecipitation of mixtures of the two (Fig. 7) eliminated the possibility that the binding was induced by effects of the substratum on either binding partner. Inhibition of biotinylated $sAPP_{695}T$ by three different non-biotinylated $sAPP_{695}$ forms (Fig. 6) suggested that neither biotinylation nor truncation of the probe produced artificial binding sites on $sAPP_{695}$. The apparent K_d for the sAPP–HKa interaction is 0.3 ± 0.1 nM determined either by $sAPP_{695}$ binding to HKa or HKa binding to $sAPP_{695}$. This is 1000-fold tighter than the binding of the HKa light chain domain 5 to urokinase receptors [35] and that of the binding of HK to negative surfaces [68]. It is also tighter than the binding of HK to endothelial cells [69] and other reported HKa–protein interactions [48–51,70].

Most biologically significant interactions are specific. HK is a large multifunctional protein composed of a 362-amino acid heavy chain, a nine-residue bradykinin domain and a 255-amino acid light chain [66]. Some functions of HK have been mapped to specific protein domains [34]. To begin to determine which region of HK contains the APP ectodomain binding site, we performed the specificity studies shown in Figs. 3 and 4. LK, a protein that lacks the light chain of HK [66] but is otherwise identical to it, did not exhibit detectable binding to $sAPP_{695}$. This is another indicator that ectodomain binding sites are contained within the light chain of HK. Further evidence is shown in Fig. 4. The light chain-containing intermediates and the light chain product, pro-

duced during plasma kallikrein processing of HK, bound $sAPP_{695}T$. These results suggest that APP may target domain 5-dependent functions of HK. Similar interactions of the light chain of HK with other proteins such as ferritin [47], thrombospondin [48], gC1q receptor [49], urokinase receptor [35], and heparin [50,51] have been reported.

The specificity of the interaction also suggests structural constraints. HKa, but not HK, bound tightly in a saturable fashion to the probe (Figs. 3, 4 and 5). We could not detect saturable binding to HK even though it contains the entire light chain (Fig. 5). This suggests that specific binding sites for $sAPP_{695}$ may be masked or inaccessible in HK. They apparently become available after HK conversion to HKa. HK undergoes conformational changes when bradykinin is released, further exposing the binding sites on its light chain [71–73]. HK is viewed as a reservoir of bradykinin [34]. It can also be viewed as a reservoir for HKa. Binding of APP to HK forms could be regulated by the amount of proteolytic processing of HK.

Our results support the idea that the $sAPP_{695}$–HKa interaction has physiological functions since colocalization of the two proteins is found in both cellular and extracellular sites in the rat brain, and that binding is specific and saturable with a low K_d occurring at physiological pH and ionic strength. When two proteins interact with each other with such high specificity, it very likely that they are involved in the same or related cellular functions [15]. The Van Broekhoven group [23], discussed the importance of binding partners of APP. These are implicated in neuronal APP functions. They noted that proteins that interact with APP may help to elucidate the physiological function and relevance of APP.

APP and HK each serve and share many functions as discussed in the Introduction. The physiological role of APP in the brain is still being assessed. At the present time, the function of HKa in the brain is unknown [39]. However, the role of HKa in angiogenesis is well documented [35]. We speculate that APP–HKa interaction could modulate neurogenesis since they both are involved in adhesion. APP facilitates neuronal adhesion while HKa (but not HK) inhibits adhesion of endothelial cells during angiogenesis. A tentative hypothesis of the APP–HKa interaction in neurons is shown in Fig. 9. This hypothesis is based on the role played by HKa in endothelial cells [35] (Fig. 9A). HKa can bind to the urokinase receptor (uPAR) on endothelial cells [45]. The urokinase receptor also binds to vitronectin with high affinity [74] promoting adhesion. Both vitronectin and HKa bind to the same site on uPAR [35]. HKa competes for binding with uPAR in the presence of vitronectin, thus displacing vitronectin from uPAR. This eventually leads to inhibition of adhesion of cells to vitronectin, thereby inhibiting angiogenesis [35]. Recent studies in our lab have shown that sAPP binds with high affinity to vitronectin (Das et al., unpublished results). Using the same analogy as shown in Fig 9A, we hypothesize that HKa and vitronectin compete for binding to sAPP and possibly also membrane-bound APP in neurons (Fig. 9B). When vitronectin binds APP, it promotes neuronal adhesion, and when HKa binds APP, it prevents adhesion thereby modulating neurogenesis. Further studies have to be carried out to determine if this hypothesis is true.

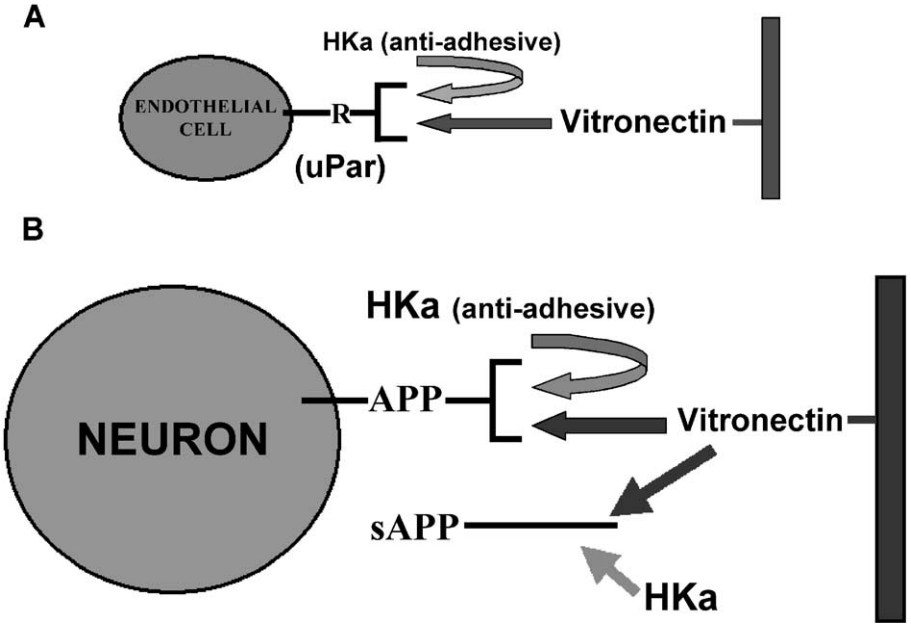

Fig. 9. Model of APP–HKa interaction. (A) Role of HKa in endothelial cells. The urokinase receptor (uPAR) participates in the control of cell adhesion and modulates angiogenesis [35]. Both HKa and vitronectin are known to compete for binding to uPAR. When vitronectin is bound to uPAR, it promotes cell adhesion, whereas bound HKa results in anti-adhesion. (B) Possible role of HKa in neurons. In this tentative hypothesis, vitronectin and HKa are pictured as competing for binding to sAPP or membrane-bound APP using the same analogy as shown in the endothelial cell in (A).

Acknowledgements

We wish to acknowledge the gift of antibodies and of the APP construct from Dr. Dennis Selkoe and Dr. Ikuro Ohsawa from the National Institute of Neuroscience, Tokyo, Japan for the gift of $sAPP_{695}$. We thank Dr. Lon Kaufman, Head, Department of Biological Sciences for departmental support, the Department of Psychiatry at the University of Illinois at Chicago for the use of laser confocal microscope and other facilities. Josepha Gomez, an undergraduate at our institution, helped us with $sAPP_{695}$ preparations and Sam Crish, a graduate student from the Neurobiology group at our institution helped us with the rat surgeries. We also want to thank Dr. Ajay K. Das for assistance with photography.

References

[1] G. Evin, K. Beyreuther, C.L. Masters, Alzheimer's disease amyloid precursor protein (AβPP): proteolytic processing, secretases and bA4 amyloid production, Amyloid: Int. J. Exp. Clin. Invest. 1 (1994) 263–280.

[2] M.P. Mattson, Cellular actions of beta-amyloid precursor protein and its soluble and fibrillogenic derivatives, Physiol. Rev. 77 (1997) 1081–1132.

[3] P.K. Panegyres, The amyloid precursor protein gene: a neuropeptide gene with diverse functions in the central nervous system, Neuropeptides 31 (1997) 523–535.

[4] G.J. Stege, G.J. Bosman, The biochemistry of Alzheimer's disease, Drugs Aging 14 (1999) 437–446.

[5] C.C. Ouimet, K.D. Baerwald, S.E. Gandy, P. Greengard, Immunocytochemical localization of amyloid precursor protein in rat brain, J. Comp. Neurol. 348 (1994) 244–260.

[6] R.B. Banati, J. Gehrmann, C. Czech, U. Monning, L.L. Jones, G. Konig, K. Beyreuther, G.W. Kreutzberg, Early and rapid de novo synthesis of Alzheimer beta A4-amyloid precursor protein (APP) in activated microglia, Glia 9 (1993) 199–210.

[7] G. Forloni, F. Demicheli, S. Giorgi, C. Bendotti, N. Angeretti, Expression of amyloid precursor protein mRNAs in endothelial, neuronal and glial cells: modulation by interleukin-1, Brain Res. Mol. Brain Res. 16 (1992) 128–134.

[8] H.A. Rohan de Silva, A. Jen, C. Wickenden, L.S. Jen, S.L. Wilkinson, A.J. Patel, Cell-specific expression of beta-amyloid precursor protein isoform mRNAs and proteins in neurons and astrocytes, Brain Res. Mol. Brain Res. 47 (1997) 147–156.

[9] M.J. Young, R.K. Lee, S. Jhaveri, R.J. Wurtman, Intracellular and cell-surface distribution of amyloid precursor protein in cortical astrocytes, Brain Res. Bull. 50 (1999) 27–32.

[10] A.I. Bush, K. Beyreuther, C.L. Masters, The beta A4 amyloid protein precursor in human circulation, Ann. N.Y. Acad. Sci. 695 (1993) 175–182.

[11] A.I. Bush, R.N. Martins, B. Rumble, R. Moir, S. Fuller, E. Milward, J. Currie, D. Ames, A. Weidemann, P. Fischer, et al., The amyloid precursor protein of Alzheimer's disease is released by human platelets, J. Biol. Chem. 265 (1990) 15977–15983.

[12] J. Ghiso, F. Tagliavini, W.F. Timmers, B. Frangione, Alzheimer's disease amyloid precursor protein is present in senile plaques and cerebrospinal fluid: immunohistochemical and biochemical characterization, Biochem. Biophys. Res. Commun. 163 (1989) 430–437.

[13] M.B. Podlisny, A.L. Mammen, M.G. Schlossmacher, M.R. Palmert, S.G. Younkin, D.J. Selkoe, Detection of soluble forms of the beta-amyloid precursor protein in human plasma, Biochem. Biophys. Res. Commun. 167 (1990) 1094–1101.

[14] R. Sherrington, E.I. Rogaev, Y. Liang, E.A. Rogaeva, G. Levesque, M. Ikeda, H. Chi, C. Lin, G. Li, K. Holman, T. Tsuda, L. Mar, J.-F. Foncin, A.C. Bruni, M.P. Montesi, S. Sorbi, I. Rainero, L. Pinessi, L. Nee, I. Chumakov, D. Pollen, A. Brookes, P. Sanseau, R.J. Polinsky, W. Wazsco, H.A.R.D. Silva, J.L. Haines, M.A. Pericak-Vance, R.E. Tanzi, A.D. Roses, P.E. Fraser, J.M. Rommens, P.H.S. George-Hyslop, Cloning of a gene bearing missense mutations in early-onset familial Alzheimer's disease, Nature 375 (1995) 754–780.

[15] S. Oliver, Guilt-by-association goes global, Nature 403 (2000) 601–603.

[16] I. Nishimoto, T. Okamoto, Y. Matsuura, S. Takahashi, Y. Murayama, E. Ogata, Alzheimer amyloid protein precursor complexes with brain GTP-binding protein G(o), Nature 362 (1993) 75–79.

[17] N. Chow, J.R. Korenberg, X.N. Chen, R.L. Neve, APP-BP1, a novel protein that binds to the carboxyl-terminal region of the amyloid precursor protein, J. Biol. Chem. 271 (1996) 11339–11346.

[18] Y. Chen, D.L. McPhie, J. Hirschberg, R.L. Neve, The amyloid precursor protein-binding protein APP-BP1 drives the cell cycle through the S–M checkpoint and causes apoptosis in neurons, J. Biol. Chem. 275 (2000) 8929–8935.

[19] F. Fiore, N. Zambrano, G. Minopoli, V. Donini, A. Duilio, T. Russo, The regions of the Fe65 protein homologous to the phosphotyrosine interaction/phosphotyrosine binding domain of Shc bind the intracellular domain of the Alzheimer's amyloid precursor protein, J. Biol. Chem. 270 (1995) 30853–30856.

[20] J.P. Borg, J. Ooi, E. Levy, B. Margolis, The phosphotyrosine interaction domains of X11 and FE65 bind to distinct sites on the YENPTY motif of amyloid precursor protein, Mol. Cell. Biol. 16 (1996) 6229–6241.

[21] M. Trommsdorff, J.P. Borg, B. Margolis, J. Herz, Interaction of cytosolic adaptor proteins with neuronal apolipoprotein E receptors and the amyloid precursor protein, J. Biol. Chem. 273 (1998) 33556–33560.

[22] P. Zheng, J. Eastman, S. Vande Pol, S.W. Pimplikar, PAT1, a microtubule-interacting protein, recognizes the basolateral sorting signal of amyloid precursor protein, Proc. Natl. Acad. Sci. U.S.A. 95 (1998) 14745–14750.

[23] G. Van Gassen, W. Annaert, C. Van Broeckhoven, Binding partners of Alzheimer's disease proteins: are they physiologically relevant? Neurobiol. Dis. 7 (2000) 135–151.

[24] D. Beher, L. Hesse, C.L. Masters, G. Multhaup, Regulation of amyloid protein precursor (APP) binding to collagen and mapping of the binding sites on APP and collagen type I, J. Biol. Chem. 271 (1996) 1613–1620.

[25] J. Caceres, E. Brandan, Interaction between Alzheimer's disease beta A4 precursor protein (APP) and the extracellular matrix: evidence for the participation of heparan sulfate proteoglycans, J. Cell. Biochem. 65 (1997) 145–158.

[26] H.J. Clarris, R. Cappai, D. Heffernan, K. Beyreuther, C.L. Masters, D.H. Small, Identification of heparin-binding domains in the amyloid precursor protein of Alzheimer's disease by deletion mutagenesis and peptide mapping, J. Neurochem. 68 (1997) 1164–1172.

[27] S. Narindrasorasak, D. Lowery, P. Gonzalez-DeWhitt, R.A. Poorman, B. Greenberg, R. Kisilevsky, High affinity interactions between the Alzheimer's beta-amyloid precursor proteins and the basement membrane form of heparan sulfate proteoglycan, J. Biol. Chem. 266 (1991) 12878–12883.

[28] M.C. Kibbey, M. Jucker, B.S. Weeks, R.L. Neve, W.E. Van Nostrand, H.K. Kleinman, beta-Amyloid precursor protein binds to the neurite-promoting IKVAV site of laminin, Proc. Natl. Acad. Sci. U.S.A. 90 (1993) 10150–10153.

[29] S. Narindrasorasak, D.E. Lowery, R.A. Altman, P.A. Gonzalez-DeWhitt, B.D. Greenberg, R. Kisilevsky, Characterization of high affinity binding between laminin and Alzheimer's disease amyloid precursor proteins, Lab. Invest. 67 (1992) 643–652.

[30] D.H. Small, H.L. Clarris, T.G. Williamson, G. Reed, B. Key, S.S. Mok, K. Beyreuther, C.L. Masters, V. Nurcombe, Neurite outgrowth regu-

lating functions of the amyloid protein precursor of Alzheimer's disease, Alzheimer's Dis. Rev. 1 (1996) 21–29.
[31] E. Storey, R. Cappai, The amyloid precursor protein of Alzheimer's disease and the Aβ peptide, Neuropathol. Appl. Neurobiol. 25 (1999) 81–97.
[32] L.W. Jin, H. Ninomiya, J.M. Roch, D. Schubert, E. Masliah, D.A. Otero, T. Saitoh, Peptides containing the RERMS sequence of amyloid beta/A4 protein precursor bind cell surface and promote neurite extension, J. Neurosci. 14 (1994) 5461–5470.
[33] A. Majumdar, A. Markaryan, B.-S. Lee, A. Kaplan, Interaction between amyloid precursor protein 695 and a light chain sequence in high molecular weight kininogen, Neurobiol. Aging 21 (1S) (2000) S117.
[34] K.D. Bhoola, C.D. Figueroa, K. Worthy, Bioregulation of kinins: kallikreins, kininogens, and kininases, Pharmacol. Rev. 44 (1992) 1–80.
[35] R.W. Colman, B.A. Jameson, Y. Lin, D. Johnson, S.A. Mousa, Domain 5 of high molecular weight kininogen (kininostatin) down-regulates endothelial cell proliferation and migration and inhibits angiogenesis, Blood 95 (2) (2000) 543–550.
[36] A.P. Kaplan, K. Joseph, Y. Shibayama, S. Reddigari, B. Ghebrehiwet, M. Silverberg, The intrinsic coagulation/kinin-forming cascade: assembly in plasma and cell surfaces in inflammation, Adv. Immunol. 66 (1997) 225–272.
[37] S. Nakanishi, Substance P precursor and kininogen: their structures, gene organizations, and regulation, Physiol. Rev. 67 (1987) 1117–1142.
[38] K. Joseph, B. Ghebrehiwet, E.I. Peerschke, K.B. Reid, A.P. Kaplan, Identification of the zinc-dependent endothelial cell binding protein for high molecular weight kininogen and factor XII: identity with the receptor that binds to the globular "heads" of C1q (gC1q-R), Proc. Natl. Acad. Sci. U.S.A. 93 (1996) 8552–8557.
[39] Z. Li, W.R. Tyor, J. Xu, J. Chao, E.L. Hogan, Immunohistochemical localization of kininogen in rat spinal cord and brain, Exp. Neurol. 159 (1999) 528–537.
[40] M. Takano, M. Horie, M. Narahara, M. Miyake, H. Okamoto, Expression of kininogen mRNAs and plasma kallikrein mRNA by cultured neurons, astrocytes and meningeal cells in the rat brain, Immunopharmacology 45 (1999) 121–126.
[41] F. van Iwaarden, P.G. de Groot, J.J. Sixma, M. Berrettini, B.N. Bouma, High-molecular weight kininogen is present in cultured human endothelial cells: localization, isolation, and characterization, Blood 71 (1988) 1268–1276.
[42] L.Y. Yung, R.W. Colman, S.L. Cooper, The effect of high molecular weight kininogen on neutrophil adhesion to polymer surfaces, Immunopharmacology 43 (1999) 281–286.
[43] L.Y. Yung, F. Lim, M.M. Khan, S.P. Kunapuli, L. Rick, R.W. Colman, S.L. Cooper, Neutrophil adhesion on surfaces preadsorbed with high molecular weight kininogen under well-defined flow conditions, Immunopharmacology 32 (1996) 19–23.
[44] L.Y. Yung, F. Lim, M.M. Khan, S.P. Kunapuli, L. Rick, R.W. Colman, S.L. Cooper, High-molecular-weight kininogen preadsorbed to glass surface markedly reduces neutrophil adhesion, Biomaterials 21 (2000) 405–414.
[45] R.W. Colman, R.A. Pixley, S. Najamunnisa, W. Yan, J. Wang, A. Mazar, K.R. McCrae, Binding of high molecular weight kininogen to human endothelial cells is mediated via a site within domains 2 and 3 of the urokinase receptor, J. Clin. Invest. 100 (1997) 1481–1487.
[46] G. Voskerician, J.M. Anderson, N.P. Ziats, High molecular weight kininogen inhibition of endothelial cell function on biomaterials, J. Biomed. Mater. Res. 51 (2000) 1–9.
[47] S.V. Torti, F.M. Torti, Human H-kininogen is a ferritin-binding protein, J. Biol. Chem. 273 (1998) 13630–13635.
[48] R.A. DeLa Cadena, E.G. Wyshock, S.P. Kunapuli, R.L. Schultze, M. Miller, D.A. Walz, R.W. Colman, Platelet thrombospondin interactions with human high and low molecular weight kininogens, Thromb. Haemost. 72 (1994) 125–131.
[49] H. Herwald, J. Dedio, R. Kellner, M. Loos, W. Muller-Esterl, Isolation and characterization of the kininogen-binding protein p33 from endothelial cells. Identity with the gC1q receptor, J. Biol. Chem. 271 (1996) 13040–13047.
[50] I. Bjork, S.T. Olson, R.G. Sheffer, J.D. Shore, Binding of heparin to human high molecular weight kininogen, Biochemistry 28 (1989) 1213–1221.
[51] Y. Lin, R.A. Pixley, R.W. Colman, Kinetic analysis of the role of zinc in the interaction of domain 5 of high-molecular weight kininogen (HK) with heparin, Biochemistry 39 (2000) 5104–5110.
[52] K. Joseph, Y. Shibayama, Y. Nakazawa, E.I. Peerschke, B. Ghebrehiwet, A.P. Kaplan, Interaction of factor XII and high molecular weight kininogen with cytokeratin 1 and gC1qR of vascular endothelial cells and with aggregated A beta protein of Alzheimer's disease, Immunopharmacology 43 (1999) 203–210.
[53] L. Bergamaschini, L. Parnetti, D. Pareyson, S. Canziani, M. Cugno, A. Agostoni, Activation of the contact system in cerebrospinal fluid of patients with Alzheimer disease, Alzheimer Dis. Assoc. Disord. 12 (1998) 102–108.
[54] I. Ohsawa, Y. Hirose, M. Ishiguro, Y. Imai, S. Ishiura, S. Kohsaka, Expression, purification, and neurotrophic activity of amyloid precursor protein-secreted forms produced by yeast, Biochem. Biophys. Res. Commun. 213 (1995) 52–58.
[55] J. Sambrook, E.F. Fritsch, T. Maniatis, Molecular Cloning: A Laboratory Manual, , 2nd edn., Cold Spring Harbor Laboratory Press, Cold Spring Harbor, NY, 1989.
[56] D.J. Selkoe, M.B. Podlisny, C.L. Joachim, E.A. Vickers, G. Lee, L.C. Fritz, T. Oltersdorf, Beta-amyloid precursor protein of Alzheimer disease occurs as 110- to 135-kilodalton membrane-associated proteins in neural and nonneural tissues, Proc. Natl. Acad. Sci. U.S.A. 85 (1988) 7341–7345.
[57] H.L. Li, J.M. Roch, M. Sundsmo, D. Otero, S. Sisodia, R. Thomas, T. Saitoh, Defective neurite extension is caused by a mutation in amyloid beta/A4 (A beta) protein precursor found in familial Alzheimer's disease, J. Neurobiol. 32 (1997) 469–480.
[58] H. Ninomiya, J.M. Roch, L.W. Jin, T. Saitoh, Secreted form of amyloid beta/A4 protein precursor (APP) binds to two distinct APP binding sites on rat B103 neuron-like cells through two different domains, but only one site is involved in neuritotropic activity, J. Neurochem. 63 (1994) 495–500.
[59] U.K. Laemmli, Cleavage of structural proteins during the assembly of the head of bacteriophage T4, Nature 227 (1970) 680–685.
[60] H. Schagger, W.A. Cramer, G. von Jagow, Analysis of molecular masses and oligomeric states of protein complexes by blue native electrophoresis and isolation of membrane protein complexes by two-dimensional native electrophoresis, Anal. Biochem. 217 (1994) 220–230.
[61] H. Schagger, G. von Jagow, Blue native electrophoresis for isolation of membrane protein complexes in enzymatically active form, Anal. Biochem. 199 (1991) 223–231.
[62] R.S. Cohen, F. Blomberg, K. Berzins, P. Siekevitz, The structure of postsynaptic densities isolated from dog cerebral cortex: I. Overall morphology and protein composition, J. Cell Biol. 74 (1977) 181–203.
[63] A. Henry, C.L. Masters, K. Beyreuther, R. Cappai, Expression of human amyloid precursor protein ectodomains in *Pichia pastoris*: analysis of culture conditions, purification, and characterization, Protein Expr. Purif. 10 (1997) 283–291.
[64] T.G. Williamson, V. Nurcombe, K. Beyreuther, C.L. Masters, D.H. Small, Affinity purification of proteoglycans that bind to the amyloid protein precursor of Alzheimer's disease, J. Neurochem. 65 (1995) 2201–2208.
[65] A.C. LeBlanc, H.Y. Chen, L. Autilio-Gambetti, P. Gambetti, Differential APP gene expression in rat cerebral cortex, meninges, and primary astroglial, microglial and neuronal cultures, FEBS Lett. 292 (1991) 171–178.
[66] Y. Takagaki, N. Kitamura, S. Nakanishi, Cloning and sequence analysis of cDNAs for human high molecular weight and low molecular

weight prekininogens: primary structures of two human prekininogens, J. Biol. Chem. 260 (1985) 8601–8609.
[67] M.A. Tayeh, S.T. Olson, J.D. Shore, Surface-induced alterations in the kinetic pathway for cleavage of human high molecular weight kininogen by plasma kallikrein, J. Biol. Chem. 269 (1994) 16318–16325.
[68] R.A. DeLa Cadena, R.W. Colman, The sequence HGLGHGHEQQHG LGHGH in the light chain of high molecular weight kininogen serves as a primary structural feature for zinc-dependent binding to an anionic surface, Protein Sci. 1 (1992) 151–160.
[69] F. van Iwaarden, P.G. de Groot, B.N. Bouma, The binding of high molecular weight kininogen to cultured human endothelial cells, J. Biol. Chem. 263 (1988) 4698–4703.
[70] A.A.K. Hasan, T. Zisman, A.H. Schmaier, Identification of cytokeratin 1 as a binding protein and presentation receptor for kininogens on endothelial cells, Proc. Natl. Acad. Sci. U.S.A. 95 (1998) 3615–3620.
[71] C.F. Scott, L.D. Silver, M. Schapira, R.W. Colman, Cleavage of human high molecular weight kininogen markedly enhances its coagulant activity. Evidence that this molecule exists as a procofactor, J. Clin. Invest. 73 (1984) 954–962.
[72] G.B. Villanueva, L. Leung, H. Bradford, R.W. Colman, Conformation of high molecular weight kininogen: effects of kallikrein and factor XIa cleavage, Biochem. Biophys. Res. Commun. 158 (1989) 72–79.
[73] J.W. Weisel, C. Nagaswami, J.L. Woodhead, R.A. DeLa Cadena, J.D. Page, R.W. Colman, The shape of high molecular weight kininogen. Organization into structural domains, changes with activation, and interactions with prekallikrein, as determined by electron microscopy, J. Biol. Chem. 269 (1994) 10100–10106.
[74] Y. Wei, D.A. Waltz, N. Roa, R.J. Drummond, S. Rosenberg, H.A. Chapman, Identification of the urokinase receptor as an adhesion receptor for vitronectin, J. Biol. Chem. 269 (1994) 32380–32388.